2016

Growth and Characterization of Molybdenum Disulfide Thin Films

Carl Morris Gross III
Wright State University

Growth and Characterization of Molybdenum Disulfide Thin Films

A thesis submitted in partial fulfillment
of the requirements for the degree of
Master of Science in Electrical Engineering

by

Carl M. Gross III
B.S.E.E., Wright State University, 2015

2016
Wright State University

Wright State University
Graduate School

May 25 2016

I HEREBY RECOMMEND THAT THE THESIS PREPARED UNDER MY SUPERVISION BY Carl M. Gross III ENTITLED Growth and Characterization of Molybdenum Disulfide Thin Films BE ACCEPTED IN PARTIAL FULFILLMENT OF THE REQUIREMENTS FOR THE DEGREE OF Master of Science in Electrical Engineering.

_____
Yan Zhuang, Ph.D.
Thesis Director

_____
Brian D. Rigling, Ph.D.
Chair, Department of Electrical Engineering
College of Engineering and Computer Science

Committee on
Final Examination

_____
Yan Zhuang, Ph.D.
Associate Professor of Electrical Engineering

_____
Shin Mou, Ph.D.

_____
Michael A. Saville, PhD, PE
Assistant Professor of Electrical Engineering

_____
Robert E. Fyffe, Ph.D.
Vice President for Research and
Dean of the Graduate School

ABSTRACT

Gross, Carl. M.S.E.E. Department of Electrical Engineering, Wright State University, 2016. *Growth and Characterization of Molybdenum Disulfide Thin Films*.

Two-dimensional materials, or materials that are only one atomic layer thick, have seen much research in recent years because of their interesting electrical properties. The first of these materials, graphene, was found to have incredible electrical properties but lacked a bandgap in intrinsic films. Without a bandgap, graphene cannot create transistors that can be shut off. Molybdenum disulfide, however, is a two-dimensional semiconductor with a large bandgap. The main issue of molybdenum disulfide is that synthesized films are a much lower quality than their exfoliated counterparts. For molybdenum disulfide to be able to be used practically, a method of synthesis must be found that can reliably create quality large area monolayer films.

In this thesis, three methods of molybdenum disulfide film synthesis are presented. Methods implemented used a tube furnace as a chemical vapor deposition system to evaporate source materials to synthesize thin films of molybdenum disulfide. An exploration into the different synthesis parameters shows optimal conditions for these specific methods. Then a discussion of these different methods is presented by judging films grown by using these methods on relevant criteria. This work shows methods to synthesize large area, polycrystalline, small grain, multilayer films, both intrinsic and doped, and to synthesize small area, single crystal and polycrystalline, monolayer films of molybdenum disulfide.

TABLE OF CONTENTS

LIST OF FIGURES

LIST OF FIGURES (cont.)

LIST OF TABLES

Acknowledgement

I would like to thank my friends, family, thesis advisor, and everyone that helped me at AFRL for all of the support during my education.

CHAPTER I

INTRODUCTION

1.1 Motivation

Life today is abundant with electronics, especially ones with computing power from cellular phones to personal computers, even some ovens and cars are being upgraded with computational abilities. Computers, at one of their lowest levels, are a number of transistors. Transistors have changed quite a bit over the years, most notably their size. In 1965, an American engineer Gordon Moore made the prediction that the number of transistors in the same amount of area will double every year: this is known as "Moore's Law" [8]. The current trend in electronics is to make circuitry smaller, and its components more densely packed, while keeping the same or better quality: speed, efficiency, or power consumption, depending on the specific application. However, this trend has come across a road block due to the materials that are currently in use. For example, silicon MOSFETs are reaching their limit because when the channel length decreases, the current while the transistor is 'off' increases, leading to lower power efficiency [9]. For current electronics to advance, new materials must be used.

Two-dimensional materials may be the key to unlock the next technological advancement. Two-dimensional materials are materials that are only one atomic layer thick. At first, two-dimensional materials were thought to only be theoretical and too unstable in the real world to be useful in any way: it was believed that the decreased

thickness would lower the melting point to impractical levels [1]. The first researched two-dimensional material, that was first isolated in 2004 by Andre Geim and Kostya Novoselov, was graphene, a flat hexagonally structured honeycomb lattice comprised of carbon atoms. After its discovery, graphene was, and still is, thoroughly researched. Through this research came the discovery of its many interesting electrical properties such as its ability to withstand much higher current densities, around six orders of magnitude, than copper, electron transport that follows Dirac-like equations, as well as other properties [1-3]. Pure layers of graphene has an absence of bandgap and field effect transistors created with graphene cannot efficiently be turned off which is why a more suitable material is need for field effect transistors (FET) [4,5].

There have been many other two-dimensional materials discovered after the discovery of graphene, like boron nitride or silicine, all with their own unique and interesting properties. One type of two-dimensional material that were discovered has attracted quite a bit of attention, transition metal dichalcogenides. Transition metal dichalcogenides layers are comprised of one transition metal atom from group IV, V, or VI and two chalcogen atoms that form two hexagonal layers of chalcogen atoms with a hexagonal layer of transition metal atoms between, where the single layers are held together via the van-der-Waals force [4, 6, 7]. These transition metal dichalcogenides have acquired much attention due to their bandgap, making them promising materials for FET devices.

The transition metal dichalcogenide that has gained the most interest is molybdenum disulfide (MoS_2). Bulk MoS_2 has been found to have an indirect bandgap of around 1.3 eV whereas its single layer form has a direct bandgap of around 1.8 eV [4,

5,7]. Bulk MoS_2 has been measured to have a room temperature mobility of around 200 $cm^2V^{-1}s^{-1}$ and fundamental n-type single layer MoS_2 has been calculated to have around 410 $cm^2V^{-1}s^{-1}$ [5]. There have been a few methods that have been proven successful in synthesizing single and few layer MoS_2 films such as thermolysis of $(NH_4)MoS_4$, sulfurization of MoO_3, and chemical vapor deposition (CVD) which has been the most practical process to synthesizing high quality, large area graphene, and other two dimensional materials [5].

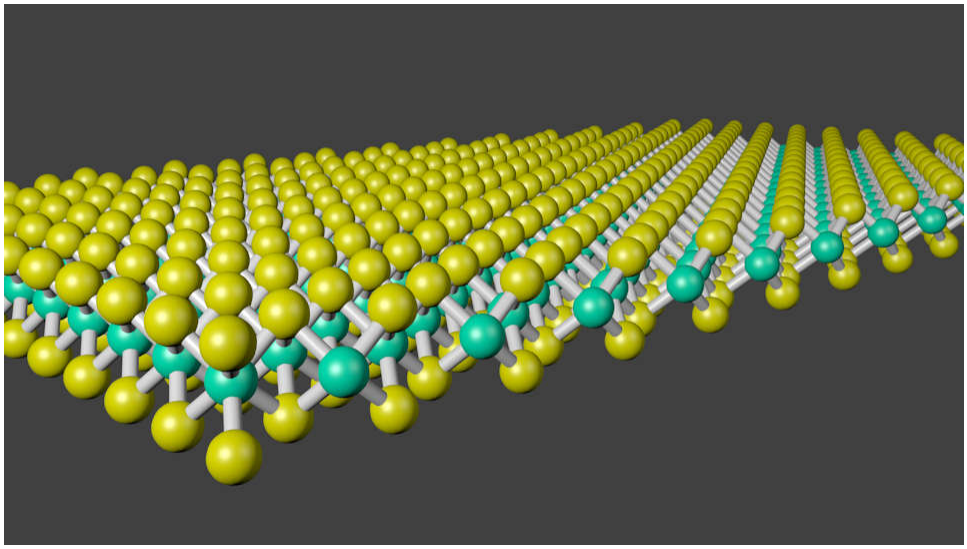

Figure 1: Three-dimensional representation of the transition metal dichalcogenide single layer structure, where the chalcogen atoms are yellow and the transition metal atoms are cyan.

1.2 Challenges

To optimize the crystal synthesis of MoS_2, there are many different variables to consider each with their own set of possible values and effects on the outcome of the sample. First, there is the materials that are used in the growth, and the amounts of those materials. Next, there is the temperature of the entire system, including the temperatures of each of the materials in the system and the times that those temperatures are achieved

and sustained. Then there is the parameters of pressure inside the system along with whether a gas is present or flowing and what the flow rate of that gas would be.

There are many different materials that have been and can be used to react and synthesize MoS_2. To successfully synthesize MoS_2, there must be a source of molybdenum and also a source of sulfur. The source of molybdenum can be anything from simple molybdenum metal to molybdenum oxide powder or even MoS_2 powder. For the sulfur source, sulfur powder or sulfur gas is generally used, but MoS_2 powder can also be used.

The temperature of the system is one of the variables that needs to be determined. Not only does the temperature of the synthesis need to be determined, but so do the temperatures of all of the materials in systems that cause the reactions to take place. Once those are determined, the ramp to those temperatures and time at those temperatures must also be determined.

The gas, or lack thereof, in the system can also affect the synthesis of the crystal. If there is enough oxygen in the system, the material that is grown will most likely not be MoS_2, which is why it is favorable to either fill the system with an inert gas, like argon, flow sulfur gas, or hold the system in a vacuum. The gas pressure is also an essential part of the synthesis process along with the flow rate of the gas, if a gas is being introduced.

The largest issue with all of these parameters is that the combination of all of these are dependent on the others. To have an optimized growth, each of these parameters must be in the correct combination, and it is possible that optimizing the individual parameters might not correspond to the completely optimize the synthesis of MoS_2.

1.3 Research Hypothesis

This work proposes an investigation into an optimized CVD process to determine the ideal method to synthesize few to single layer MoS_2 for electronic applications. Presently, there is no optimal synthesis method to create MoS_2. One of the popular methods of synthesizing MoS_2 is to heat sulfur powder and a powder containing molybdenum or molybdenum disulfide powder into a vapor to have them deposit onto a substrate. During this synthesis, the following reaction occurs:

$$2MoO_3(\text{vapor}) + 2S_2(\text{vapor}) \rightarrow 2MoS_2(\text{on substrate}) + 3O_2(\text{gas})$$

Another popular method to synthesize MoS_2 onto a substrate is to first deposit molybdenum metal onto the substrate and then to heat a powder that includes sulfur to sulfurize the film. The reaction that occur during this synthesis is the following:

$$Mo\ (\text{on substrate}) + S_2(\text{vapor}) \rightarrow MoS_2(\text{on substrate})$$

There are many methods that will produce MoS_2, however not all of these will produce the quality of crystal that the others. To produce the highest quality of crystal that can be synthesized, the many parameters must be at their optimal values. These parameters include temperature of all material, time to and at temperature, pressure, gas flow rate, and the amount of the various materials used.

1.4 Thesis Outline

Chapter II provides context for methods and equipment used for crystalline growth and characterization. Chapter III presents the results of the characterizations done unto the created samples. Chapter IV proposes conclusions and outlook for future work.

CHAPTER II

EXPERIMENTS

When molybdenum disulfide started becoming popular among researchers, many different methods were implemented to attempt to synthesize large-area (millimeter or larger scale) films that had the qualities of mechanically exfoliated samples (which cannot be used for practical purposes) or higher. MoS_2 films have been synthesized by chemical vapor deposition (CVD) using precursors such as MoO_3, MoO_2, $MoCl_5$, Mo, and $(NH_4)MoS_4$, sulfurization of MoO_3, thermolysis of $(NH_4)MoS_4$, physical vapor deposition, and hydrothermal synthesis [5, 10, 11]. Though all of these methods have their own advantages, CVD seems to be the key to large-area high-quality MoS_2.

2.1 Chemical Vapor Deposition System

Deposition is the state change of matter in which a gas or vapor solidifies. A CVD process is a chemical procedure designed to deposit a chemical onto a substrate. CVD systems are used often to produce high-performance, high quality materials and is popular in the production of thin films. CVD systems can be used to deposit materials in amorphous, polycrystalline, monocrystalline, and epitaxial forms. Generally, this is done by heating a chemical to the point of evaporation and letting the vapor solidify onto a desired substrate. Sometimes it is advantageous to have multiple vapors react and deposit a desired combination of the vapors' elements onto the substrate.

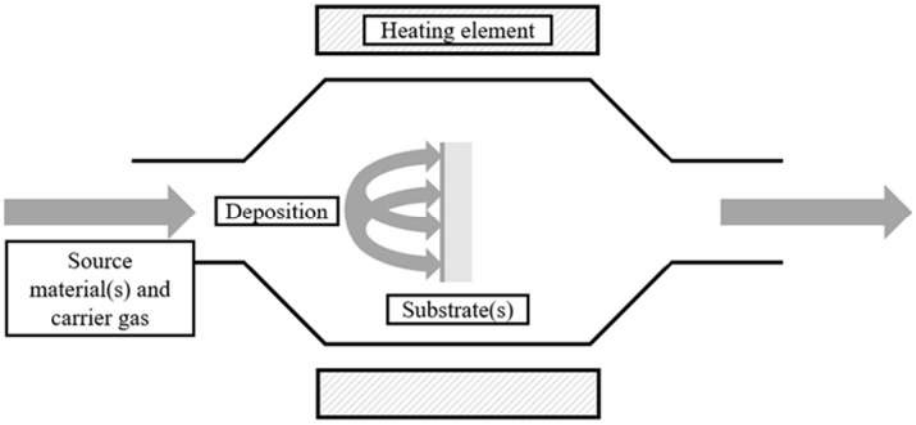

Figure 2: Diagram of a simple chemical vapor deposition system.

CVD has been proven to be one of the most practical methods of high quality, large-area films of graphene [5]. Before 2009, graphene was faced with the same issue that molybdenum disulfide is facing now, finding a method to produce large-area high quality and uniform films [12]. In 2009, a technique was found where graphene could be grown by CVD of carbon onto copper foil using a mixture of methane and hydrogen at temperature up to 1000° C produced high quality large-area graphene that was able to be transferred off the copper foil it was grown onto [12]. This completely changed the market of graphene: now, most graphene on the market was grown using a similar CVD method. Then, CVD was found to be a practical method of producing other similar materials such as boron nitride and BCN nanosheets [5]. Recent experiments report promise to lead to synthesis of large-area high-quality MoS_2 films with controllable number of layers [4].

Even though CVD synthesis has occurred, this is still a fairly new process and the largest problem facing the practical viability of MoS_2 is that the polycrystalline films produced have been inferior to exfoliated flakes which is possibly due to the effects of the grain boundaries [5]. To combat this challenge, various aspects of the growth must be

optimized. There are many parameters that can affect the synthesis of a MoS_2 film such as growth temperature, temperature of the source materials, temperature rate of change, growth time, pressure, carrier gas flow rate, and, of course, the source material themselves. Another aspect that could be explored is seeded growth, which solved this issue for graphene synthesis, which is a chemical that promotes the nucleation of crystal growth [5].

2.2 Experimental Setup

A tube furnace structure is a simple system that can be used for a CVD process that allows for the control of parameters of the growth that are important for the synthesis of high-quality MoS_2 films. Tube furnace systems are made commercially to hold and heat a tube to a desired temperature for specific amounts of times, can be held at specific pressures (vacuum or higher pressures), have different temperature regions, and also increases the repeatability of experiments with lower chance of inconsistencies. The tube furnace that this experiment uses is a Thermo Scientific™ Lindberg/Blue M™ Mini-Mite™ Model TF55030A-1. This tube furnace is programmable with a microprocessor-based self-tuning PID controller to reach certain temperatures in given times without overshooting [13]. It is also made to heat a 1 inch (2.54 cm) diameter tube to a temperature range of 100º to 1100ºC and is insulated with Moldatherm [13].

Some of the most important growth parameters are pertaining to the heat profile. These parameters include growth temperature, temperature rate of change, temperature of source material(s), and growth time. These parameters are why it is important to be able to program a heat profile for consistency and specificity to change exact parameters. It

has been reported that MoS_2 films have been grown at temperatures ranging from 650° C to 1100° C.

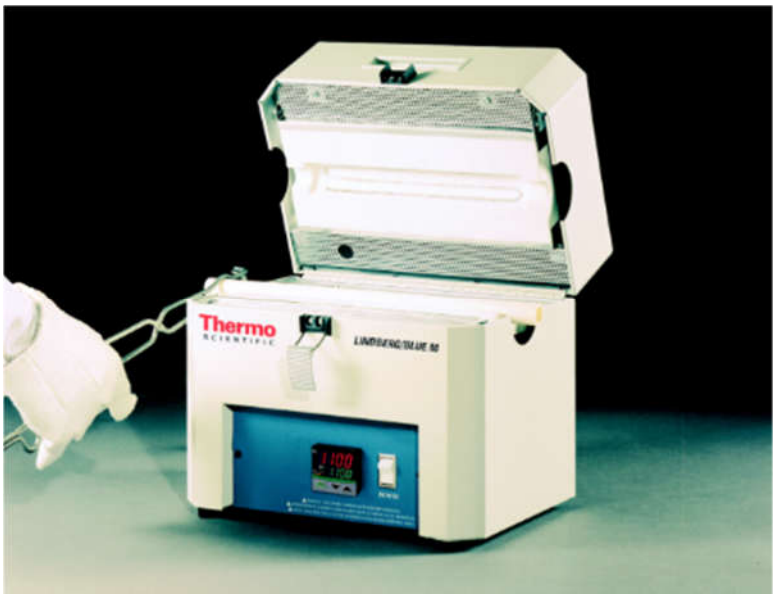

Figure 3: Thermo Scientific™ Lindberg/Blue M™ Mini-Mite™ Model TF55030A-1 Tube Furnace [13].

The heat profile of the tube furnace is programmed by setting variables on the controller. First a starting temperature is assigned to the controller, this is the temperature at which the system is assumed to start at. Temperature set points are then assigned to the controller associated with corresponding time durations to reach those set points. Next, alarms are set so that if the system gets to a certain temperature, the alarm will sound and the furnace will no longer heat. Finally, option is given to have the program either repeat, dwell on the last temperature set point, or shut off after the system has completed its program. The temperature sensor of the tube furnace is in the center of the heated area and can measure the temperature of the tube at that point. Since the tube is longer than the heated area, the areas closer to the outside of the heated areas are different temperatures than the center of the tube, creating various heat profiles for different points inside the tube.

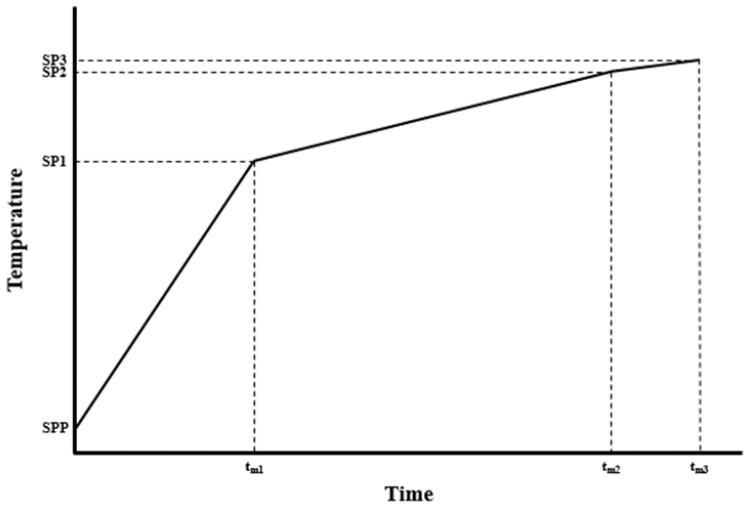

Figure 4. Example heat profile temperature versus time.

The above figure, Figure 4, is an example of what a heat profile of a tube furnace might look like. SPP designates the starting temperature of the system while SP1, SP2, and SP3 designate the temperature set points in the heat profile. t_{m1}, t_{m2}, and t_{m3}, correspond with the temperature set points as time periods to reach their respective temperatures. Having a slower ramping of the temperature helps stabilize the temperature inside to tube and help keep the more of the tube at a uniform temperature.

To control the system, the tube is first purged using a vacuum pump that achieves 5 mTorr (~0.667 Pa) then is filled with technical grade argon of 99.997% purity, as an inert gas. This process happens five times to ensure any contaminants in the tube are removed from the system. After that, the carrier gas (argon) flow and system pressure is manually set by the valve at the outlet along with the pressure regulator on the argon cylinder. The tube is then allowed to continuing purging by the flow of argon for thirty minutes before the heating process begins. Having a lower carrier gas flow rate keeps the source chemicals of the growth inside the system while also decreasing the likelihood of outside contaminants interfering with the synthesis process. Crystallinity of the film and

density of nucleation sites are both affected by the pressure inside the system [14]. Increased pressure, decreases the amount of source material evaporated which slows the synthesis process [14]. Pressure can even affect the grain size, and area coverage of the film growth [14].

The CVD system set up in this experiment uses a one inch diameter quartz tube, tube flanges, O-rings, tube blocks, and quartz crucibles from MTI Corporation. Elemental sulfur powder (≥99% purity), which has a boiling point of 444.6° C, is used as the sulfur source for the molybdenum disulfide growth, and molybdenum(VI) oxide (MoO_3) powder (≥99% purity) or molybdenum metal sputtered on the substrate is used as the molybdenum source. The reactions that synthesizes the films with those sources is

$$2MoO_3(\text{powder}) + 2S_2(\text{powder}) + \text{heat} \rightarrow 2MoO_3(\text{vapor}) + 2S_2(\text{vapor}) + \text{heat} \rightarrow 2MoS_2(\text{on substrate}) + 3O_2(\text{gas})$$ and

$$2MoO_3(\text{powder}) + 2S_2(\text{powder}) + \text{heat} \rightarrow 2MoO_3(\text{vapor}) + 2S_2(\text{vapor}) + \text{heat} \rightarrow 2MoS_2(\text{on substrate}) + 3O_2(\text{gas})$$, respectively.

Since the environment inside the system is controlled, this is the only reaction that occurs. This reaction is chemical limited growth controlled by the placement of the source materials. Since the CVD system has different temperature zones, placing the source materials at different positions in the tube will control the temperature of the substrate when the reaction occurs. To optimize the synthesis methods, the variables that appeared to be the most important, such as the temperature of the materials, were varied while all of the other growth parameters were kept constant. After the variable sweep, the samples would be compared to find the optimal method.

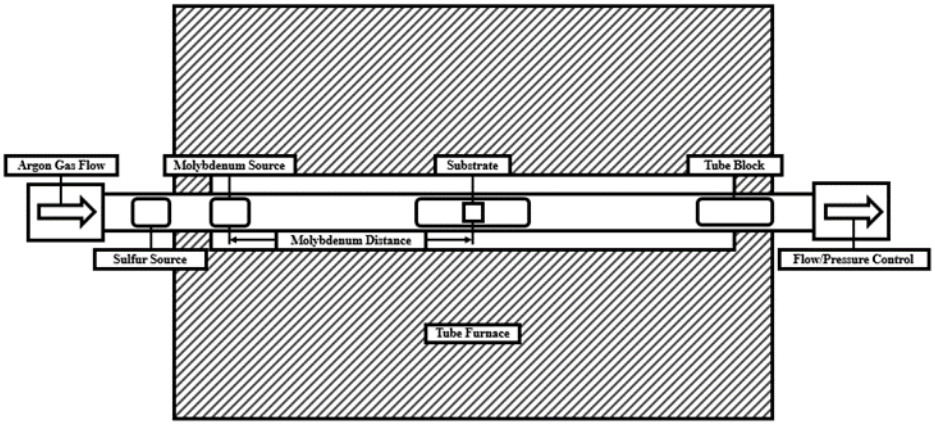

Figure 5. Diagram of the CVD system.

The temperature is measured in the center of the tube, this is where the temperature in the system matches the temperature set by the program of the tube furnace. Since the insulation of the furnace is not perfect and the temperature outside of the furnace is much lower than the inside of the furnace, a temperature gradient is created. While the center of the tube, where the sample is located and the film is grown, is uniformly heated, the temperature is lowered as the distance from the center is increased. This temperature gradient, while not affecting the sample, helps control the amount of source material vapor inside the tube. By setting the source materials further away from the center of the tube, the temperatures reached by those materials is decreased, decreasing the amount of the material that is evaporated. By tuning this method of chemical limiting, it is possibly to control the thickness of the film.

2.3 Characterization Techniques

Impurities are a large part of the field of materials, whether the impurities are intentional or not intentional. To determine the quality of films that have been grown,

various characterization techniques must be utilized. Raman spectroscopy can be used to lend some insight into the molecular structure of the film. Hall Effect measurement can be used to determine properties such as electron and hole concentration as well as electron and hole mobility. Sheet resistivity measurements can be used to measure some of the effects of doping or unintentional impurities.

Raman spectroscopy uses the scattering of light, generally a laser of a specific frequency in the near infrared to near ultraviolet range, to detect low-frequency modes, such as vibrational modes, of a subject. The energy of the photons from the laser reacts with the molecular vibrations of the subject and shifts the energy either up or down, providing information about the molecular structure in relation to its low-frequency modes. The information procured from Raman spectroscopy can be used to identify the molecular make-up of a sample since the vibrational modes can be directly related to specific chemical bonds and symmetries that could be present in the molecular structure. Instead of reporting the energy shift from the vibrational modes, Raman shift is measured in wavenumbers which are directly linked to the energy shift, generally in units of inverse centimeters.

The equipment this experiment uses to perform the Raman spectroscopy to characterize the molybdenum disulfide samples is a Renishaw InVia Raman Microscope using a 532 nm wavelength laser excitation source. MoS_2 crystals have two characteristic modes found through Raman spectroscopy: E_{2g}^1, the in-plane vibration of sulfides, and A_{1g}, the out-of-plane vibration of sulfides [5]. These peaks in intensity can provide information that can suggest crystalline quality. If the peaks have smaller full width at half maximums (FWHM), it can be assumed that the crystalline quality is higher than a

sample with larger FWHMs [16]. The intensity peaks of E_{2g}^1 and A_{1g} are generally located at around 383 cm^{-1} and 405 cm^{-1}, respectively, although it has been stated that the difference of the wavenumber between these two peaks can express the number of MoS_2 layers present, where a smaller difference suggests fewer layers [5]. The peak difference suggesting number of layers is around 20 cm^{-1} for single layer, and around 22 cm^{-1} for bilayer [5]. Using Raman spectroscopy is an adequate way to, non-destructively, determine the crystalline quality and thinness of MoS_2 films and grains.

The Hall Effect is observed when a magnetic field is applied through a sample as well as a current is running across the sample. The Lorentz force, the force applied to a moving charge particle from a magnetic field, causes the magnetic field and current to create another current perpendicular to both, which also creates a voltage, or Hall voltage [15]. Hall Effect measurement system is used to determine Hall voltage, but can also be used to derive information such as carrier mobility, carrier concentration, Hall coefficient, resistivity, magnetoresistance, and conductivity type [15]. This experiment implemented the van der Pauw method of measuring the Hall Effect. This method places four contacts, for this experiment, on the corners of the 1 cm square sample and measuring the voltage across two adjacent terminals when a current is introduced in the other two adjacent terminals both with and without the magnetic field present [16]. The Hall Effect system used in this experiment is a non-commercial system that can go to high temperatures (~400° C), which the system measures accurately to the thousandth of a degree, and can produce a magnetic field of around 3 T, which the system measures accurately to the thousandth of a Tesla. Then a computer takes the information from all of the voltage, current, magnetic field, and temperature

measurement devices and, through the use of a noncommercial LabVIEW program, outputs the calculated information.

Figure 6. Illustration of Hall Effect [15].

Accurate resistivity measurements are usually made by four equally-spaced collinear probes. The outer probes provide a current while the inner probes measure voltage. The use of this four-probe measurement instead of the traditional two-probe measurement eliminates the parasitic voltage drops such as probe and contact resistances as well as eliminating the issue of current spreading [16].

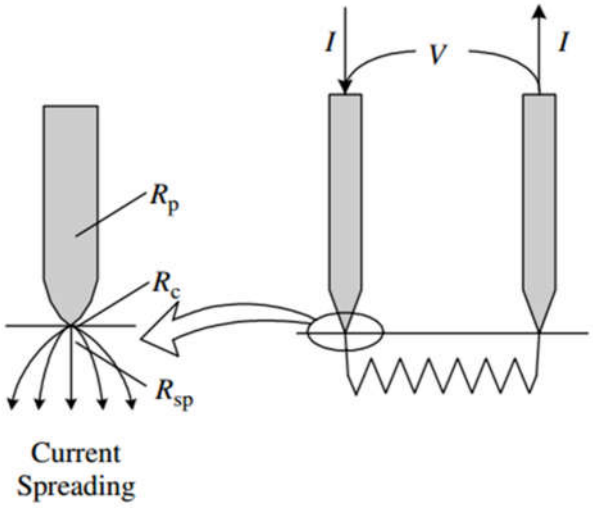

Figure 7. Two-probe arrangement showing the probe resistance R_p, the contact resistance R_c and the spreading resistance R_{sp} [16].

Resistivity from a four-probe measurement, for a sample under ideal conditions with infinite length, width, and thickness, and no shape or edge factors can be found by

$$\rho = \frac{2\pi}{\left(\frac{1}{s_1} \quad \frac{1}{s_1 + s_2} \quad \frac{1}{s_1 + s_2} + \frac{1}{s_3}\right)} \frac{V}{I} \text{ [16]}$$

Where ρ is resistivity, V is the difference in voltages measured in probe two and probe three, I is the current through probe one and four, s_1 is the distance between probe one and two, s_2 is the distance between probe two and three, and s_3 is the distance between probe three and four. When the probes are place equally spread apart at distance s the equation then becomes

$$\rho = 2\pi s \frac{V}{I} \text{ [16]}$$

To become corrected for the geometry of the sample being finite and arbitrarily shaped, the correction factor F is multiplied to correct for probe location, thickness, sample diameter, and temperature. For thickness of the sample, t, less than half of the probe spacing, the corrected resistivity equation becomes

$$\rho = \frac{\pi}{\ln(2)} t \frac{V}{I} \approx 4.532 t \frac{V}{I} \text{ [16]}$$

Samples than are extremely thin are generally characterized using sheet resistance, R_{sh}, instead of resistivity given by

$$R_{sh} = \frac{\rho}{t} = \frac{\pi}{\ln(2)} \frac{V}{I} \approx 4.532 \frac{V}{I} \text{ [16]}$$

The instrument used to perform resistivity measurements in this experiment, a Keithley 4200 Semiconductor Characterization System.

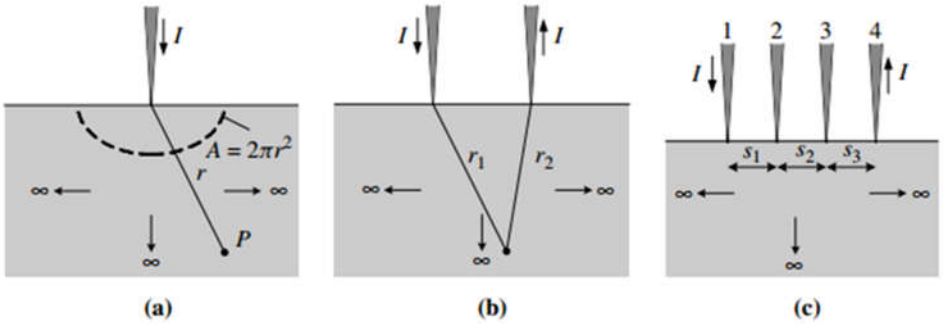

Figure 8. (a) one-point probe, (b) two-point probe, and (c) collinear four-point probe showing current flow and voltage measurement [16].

Another four probe measurement that can be used is called the van der Pauw method which can be more accurate and can be used on arbitrary shapes [16]. By placing four sufficiently small contacts, call them 1, 2, 3, and 4 in that order, around the entire outside of a sample of uniform thickness, the resistance $R_{12,34}$ is defined as $R_{12,34} = \frac{V_{34}}{I_{12}}$ where I_{12} is the current that enters 1 and leaves 2 and $V_{34}=V_3-V_4$ which is the voltage difference of 3 and 4 [16]. Then resistivity can be found to be $\rho = \frac{\pi}{\ln(2)} t \frac{R_{12,34}+R_{23,41}}{2} F$ but is a sample is symmetric, the resistance can be simplified to

$$\rho = \frac{\pi}{\ln(2)} t R_{12,34} \sim 4.532 t R_{12,34}$$ [16].

CHAPTER III

RESULTS

3.1 Sputtered Molybdenum Metal

The main difference of the methods explored in this work is the molybdenum source. The first method implemented used 5nm of sputtered molybdenum metal deposited on the sample the molybdenum source, then was sulfurized though evaporating around 0.6g of elemental sulfur powder through heating at set temperatures. 5nm was chosen as a repeatable method to obtain a thin, continuous layer of molybdenum to create a continuous film of molybdenum disulfide. The blank 1cm by 1cm sample was given to someone who has calibrated this sputtering method to consistently create a consistent 5nm film across the whole surface of the sample. 0.6g of elemental sulfur powder was chosen as an amount of sulfur to consistently evaporate during the growth process and to fully sulfurize the layer of molybdenum metal. The heat of the substrate and the sulfur vapor within the system causes the sulfur vapor to combine with the molybdenum metal on the surface of the substrate to create molybdenum disulfide. All films created through this method were synthesized on a silicon substrate with a 300nm layer of polished, thermally grown SiO_2 on top.

As shown in Figure 9, the temperature profile in the center of the tube, after the environment of the system was controlled by filling the tube with argon (and getting rid of any other gas in the tube by vacuum), reached 550° C in thirty minutes, and then

reached the growth temperature, which was changed for different samples, after that. The temperature was then held at the growth temperature for fifteen minutes and then cooled naturally back to room temperature. Fifteen minutes was chosen to evaporate nearly all of the sulfur powder so that sulfur vapor would be continuously in the system for the entire process. All experiments used argon as a carrier gas with a flow rate of around 200 sccm (standard cubic centimeters per minute). Argon was chosen as the carrier gas because argon is an inert gas that would not interact with the synthesis process. Each sample was grown at atmospheric pressure. The crucible of elemental sulfur was placed in the tube so that sulfur gas would be flowing through the tube when the system reached growth temperature.

Raman spectroscopy of the samples grown at 650° C, 700° C, 750° C, and 850° C are shown in Figures 10, 11, 12, and 13, respectively. From the data from the Raman spectroscopy, clear E_{2g}^1 and A_{1g} peaks are present along with silicon's (the substrate) Raman peak around 520 cm^{-1}. Table 1 is a table showing the locations of the E_{2g}^1 and A_{1g} peaks along with the difference between them (A_{1g}- E_{2g}^1) for each sample.

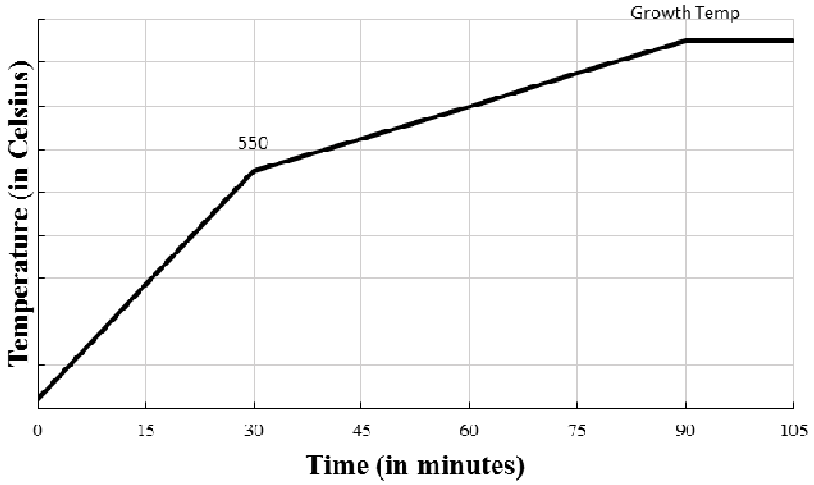

Figure 9. The temperature profile of the sputtered molybdenum samples.

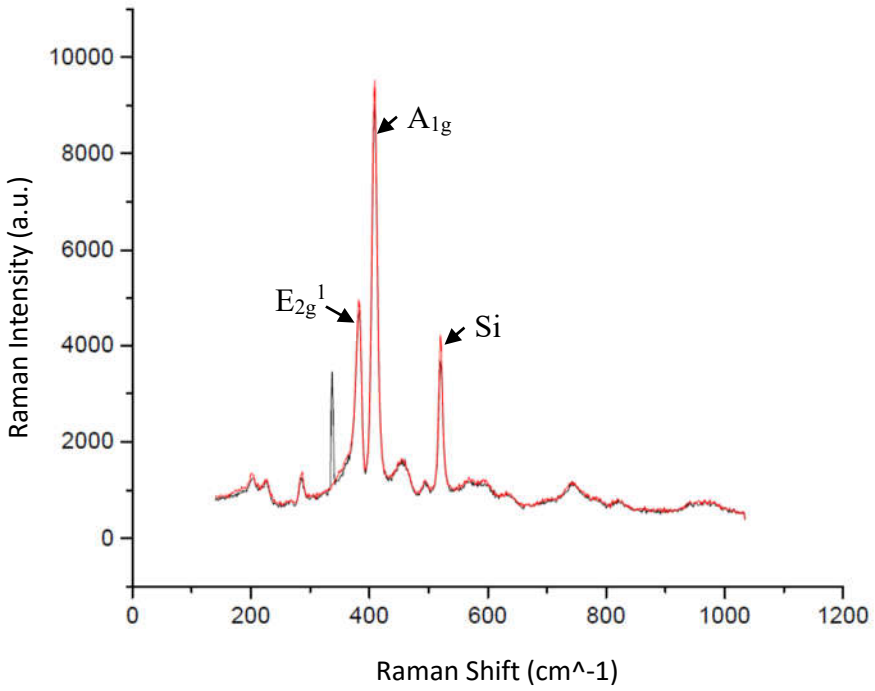

Figure 10. Raman spectrum of MoS_2 sample grown at 650° C by sputtered molybdenum.

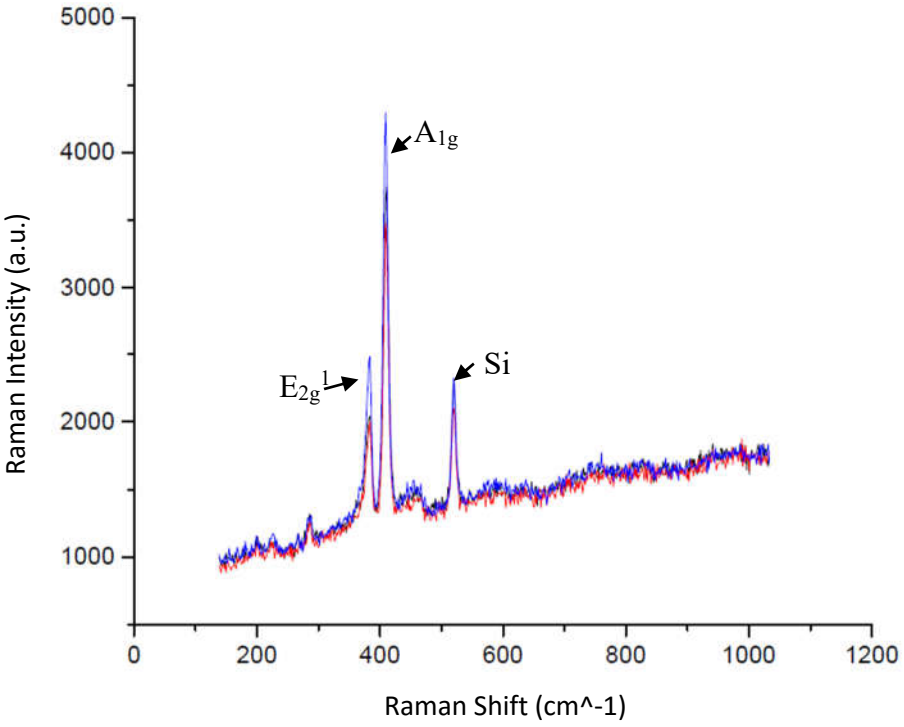

Figure 11. Raman spectrum of MoS_2 sample grown at 700° C by sputtered molybdenum.

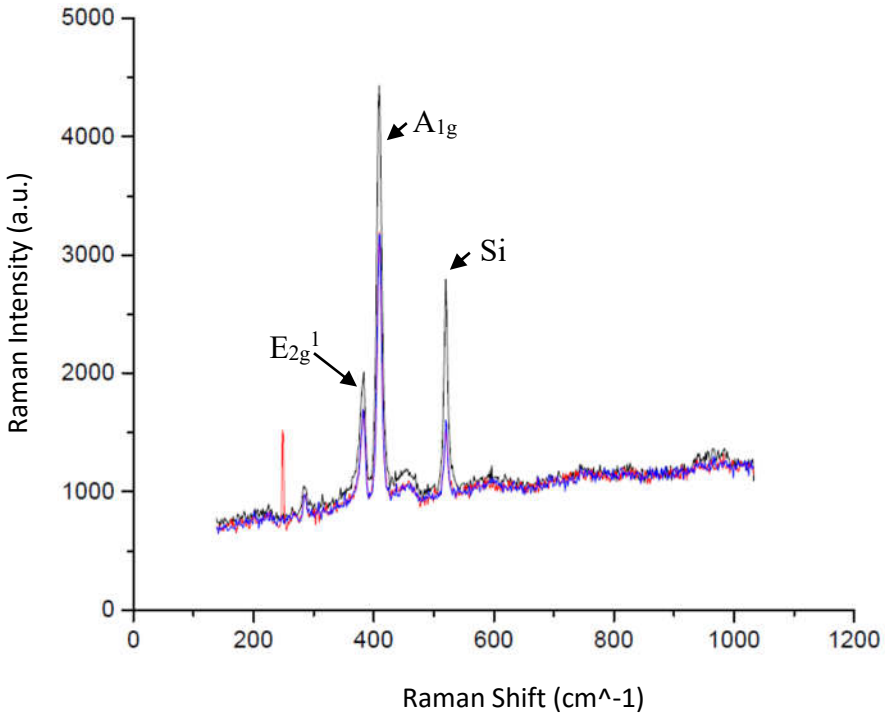

Figure 12. Raman spectrum of MoS_2 sample grown at 750° C by sputtered molybdenum.

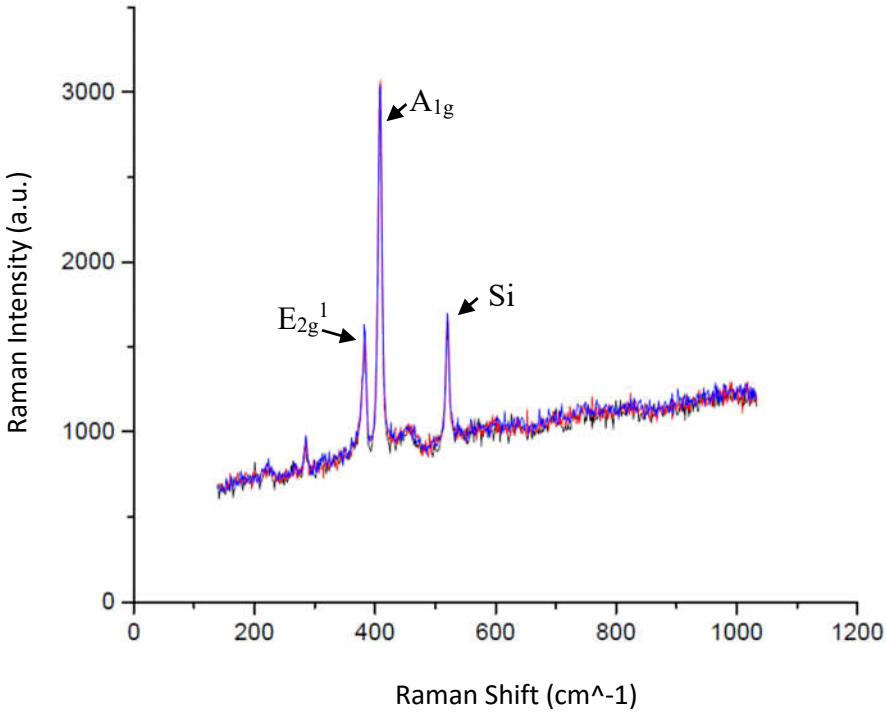

Figure 13. Raman spectrum of MoS_2 sample grown at 850° C by sputtered molybdenum.

Growth Temp (℃)	E_{2g}^1 Location (cm^{-1})	A_{1g} Location (cm^{-1})	Difference (cm^{-1})
650	383.761	409.325	25.564
700	383.648	410.807	27.159
750	383.592	409.157	25.565
850	383.592	409.157	25.565

Table 1. Raman peak locations for MoS_2 samples grown by sputtered molybdenum at different temperatures.

This method proved to be a fairly simple and highly repeatable way to synthesize large area films of molybdenum disulfide. As the Raman spectrums show, samples grown at these different growth temperatures produce similar films. The full-width half-maximums of the samples show a slight trend of thinner peaks (specifically the A_{1g} peak) at higher temperatures, from about $15cm^{-1}$ to about $11cm^{-1}$. The peak differences of the differently grown samples are all between $25cm^{-1}$ and $28cm^{-1}$ which means these films are multilayered [5]. There are also multiple peaks within the Raman spectrums that are not specific to molybdenum disulfide or silicon, this shows that there are impurities within the synthesized films. These impurities could be due to oxygen content within the system, creating molybdenum oxysulfide. These samples under an optical microscope showed no visible features or grains, leading to the conclusion that the grains produced were below the microscope's detection limit, making the exact size and shape of the grains unable to be determined, and therefore the sample could be considered polycrystalline. In conclusion, a simple exploration into this method showed repeatable,

large area, multilayer molybdenum disulfide that was not highly affected by changing variables within the synthesis process. The Raman shows that all of the thicknesses of the samples are similar, all of the samples being more than three layers thick, but it also shows that the full-width half-maximum of the samples grown at 850° C is less than the other samples grown at other temperatures that can mean is has higher crystallinity.

3.2 Sputtered Molybdenum Metal with Intentional Niobium Impurities

One of the biggest issues facing synthesized molybdenum disulfide for electronics, is the high sheet resistivity. This high resistance is due to the grain boundaries present in polycrystalline films. Because of the polycrystalline nature of the films grown in 3.1, introducing niobium impurities, which acts like an acceptor, could decrease the sheet resistance, and therefore increase the efficiency of devices that would be created from these films [18]. To introduce the niobium into the synthesis process, the preparation of the sample prior to the sulfurization was slightly changed. The blank 1cm by 1cm sample was given to someone who has calibrated this sputtering method to consistently create a consistent 2.5nm film of molybdenum metal across the whole surface of the sample, then created a 2.5nm film of niobium metal across the whole surface, then again with molybdenum metal creating three 2.5nm layers on top of the blank sample as shown in Figure 14. Through the same sulfurization methods as implemented previously, the new films were doped with niobium metal 0.6g of elemental sulfur powder was chosen as an amount of sulfur to consistently evaporate during the entire growth process and to sulfurize the layers of molybdenum and niobium metals. The heat of the substrate and the sulfur vapor within the system causes the sulfur vapor to

combine with the molybdenum metal on the surface of the substrate to create molybdenum disulfide. All films created through this method were synthesized on a silicon substrate with a 300nm layer of polished thermally grown SiO_2 on top.

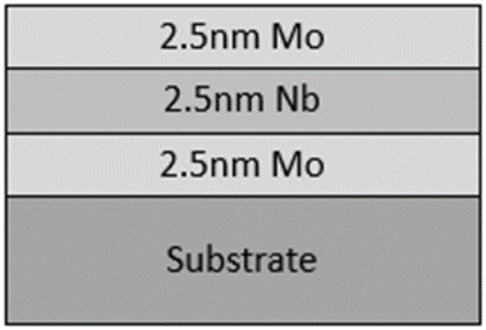

Figure 14. Diagram of the sample before sulfurization (not to scale).

As shown in Figure 9, the temperature profile, like the previous set of samples, in the center of the tube, after the environment of the system was controlled, reached 550° C in thirty minutes, and then reached the growth temperature, which was changed for different samples, after that. The temperature was then held for fifteen minutes and then cooled naturally back to room temperature. Fifteen minutes was chosen to evaporate nearly all of the sulfur powder so that sulfur vapor would be continuously in the system for the entire process. All experiments used argon as a carrier gas with a flow rate of around 200 sccm (standard cubic centimeters per minute). Argon was chosen as the carrier gas because argon is an inert gas that would not interact with the synthesis process. Each sample was grown at atmospheric pressure. The crucible of elemental sulfur was placed in the tube so that sulfur gas would be flowing through the tube when the system reached growth temperature.

Raman spectroscopy of the samples grown at 850° C, 900° C, 950° C, and 1000° C are shown in Figures 15, 16, 17, and 18, respectively. Within the data from the Raman

spectroscopy, clear E_{2g}^1 and A_{1g} peaks are present along with silicon's (the substrate) Raman peak around 520 cm^{-1}. Table 2 is a table showing the locations of the E_{2g}^1 and A_{1g} peaks along with the difference between them (A_{1g}- E_{2g}^1) for each sample. Table 3 shows the measured sheet resistances of each of the doped samples.

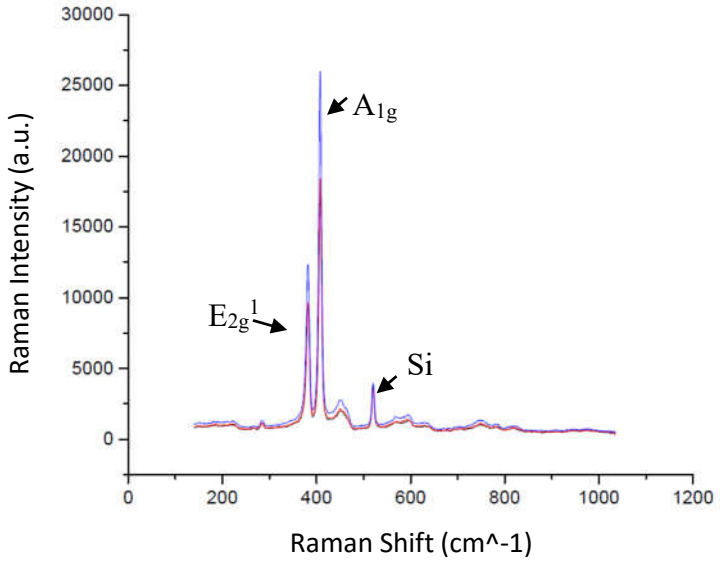

Figure 15. Raman spectrum of MoS_2 sample grown at 850° C by sputtered molybdenum and niobium.

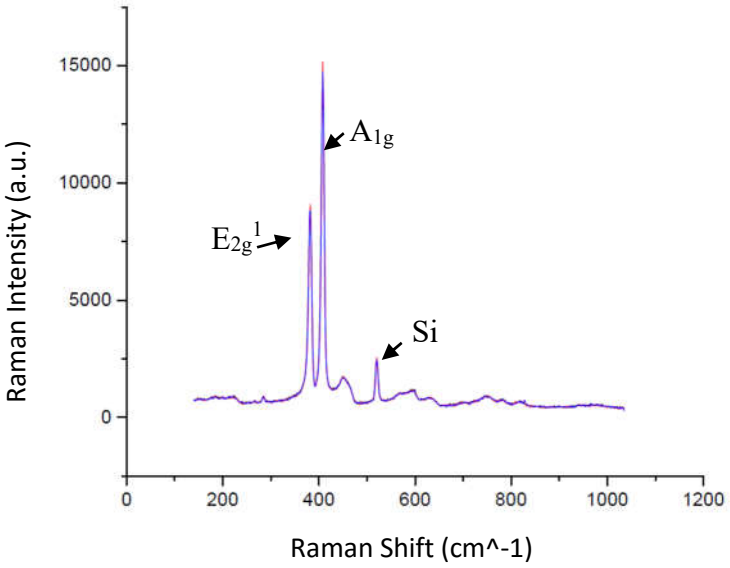

Figure 16. Raman spectrum of MoS_2 sample grown at 900° C by sputtered molybdenum and niobium.

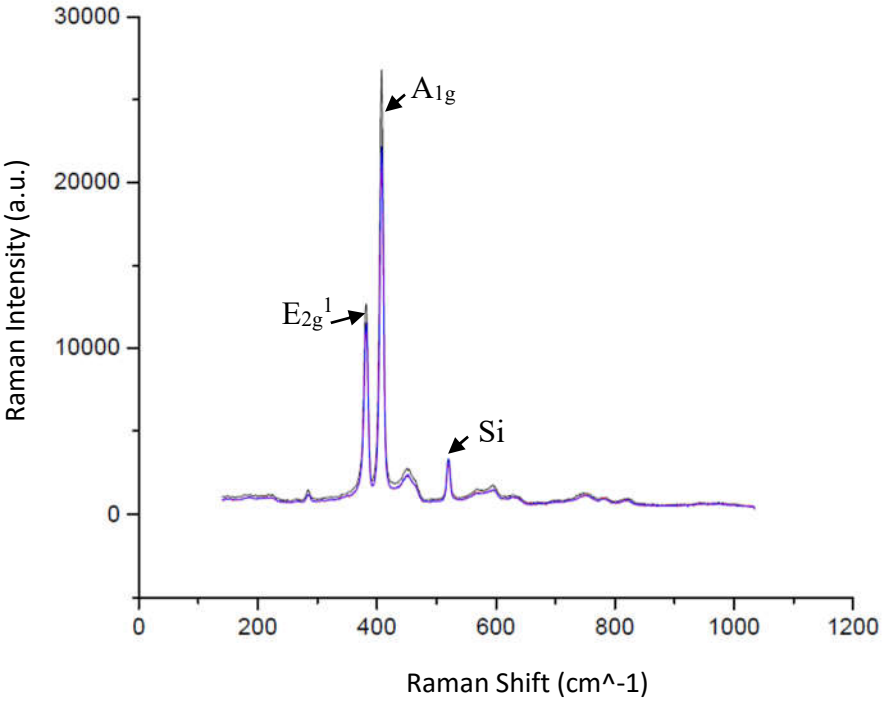

Figure 17. Raman spectrum of MoS_2 sample grown at 950° C by sputtered molybdenum and niobium.

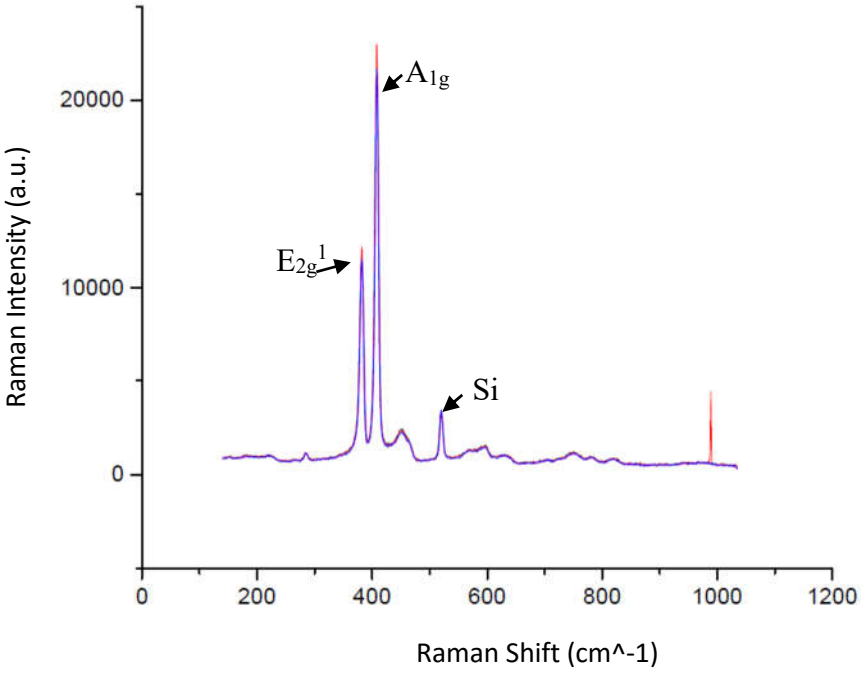

Figure 18. Raman spectrum of MoS_2 sample grown at 1000° C by sputtered molybdenum and niobium.

Growth Temp (℃)	E_{2g}^1 Location (cm^{-1})	A_{1g} Location (cm^{-1})	Difference (cm^{-1})
850	382.339	407.907	25.568
900	382.339	407.907	25.568
950	382.339	407.907	25.568
1000	382.339	407.907	25.568

Table 2. Raman peak locations for MoS_2 samples grown by sputtered molybdenum and niobium at different temperatures.

Growth Temperature (in ℃)	Sheet Resistance (in kΩ/Square)
850	330
900	35
950	150
1000	540

Table 3. Resistivity of Nb doped MoS_2 samples at different growth temperatures.

This method, similar to the previous method, proved to be a fairly simple and highly repeatable way to synthesize large area films of molybdenum disulfide with niobium impurities. As the Raman spectrums show, samples grown at these different growth temperatures produce similar films. The full-width half-maximums of the samples do not show any specific trends with these sets of films. The peak differences of the differently grown samples are all 25.568cm^{-1} which means these films are multilayered [5]. There are also multiple peaks within the Raman spectrums that are not specific to molybdenum disulfide or silicon, this shows that there are other impurities within the

synthesized films. These impurities could be due to oxygen content within the system, creating molybdenum oxysulfide. These samples under an optical microscope showed no visible features or grains, leading to the conclusion that the grains produced were below the microscope's detection limit, making the exact size and shape of the grains unable to be determined, and therefore the sample could be considered polycrystalline. The resistance study, using four probe measurements as discussed in the previous chapter, of the various samples grown at different temperatures show that the sample grown at 900° C had the lowest sheet resistance by about a magnitude of 4. In conclusion, a simple exploration into this method showed repeatable, large area, polycrystalline, multilayer molybdenum disulfide with niobium impurities with a sheet resistance that was affected by the growth temperature. The Raman shows that all of the thicknesses of the samples are similar, all of the samples being more than three layers thick, but the sample grown at 900° C had the lowest sheet resistance. For what this experiment was trying to accomplish, the growth conditions for the samples grown at 900° C are the optimal growth conditions.

3.3 Molybdenum(VI) Oxide Powder

Another way to try to solve the issue of resistance is to lower the number of grain boundaries. To accomplish this goal, the films grown must be polycrystalline with larger crystals or single crystalline structure rather than polycrystalline with smaller crystals. One way to do this is to this is to grow the crystals on a clean substrate, meaning nothing present of the surface of the substrate. The final method that was implemented used molybdenum(VI) oxide powder in a crucible as a molybdenum source rather than

sputtered molybdenum metal on the sample. The sample would go into the system without anything on its surface and, using different set temperatures, would nucleate molybdenum disulfide crystals on its surface using the evaporated molybdenum(VI) oxide (~0.03g) and elemental sulfur (~0.6g) powders, the chemical reaction that occurs was described in the previous chapter.

As shown in Figure 9, the temperature profile, like the previous set of samples, in the center of the tube, after the environment of the system was controlled, reached 550° C in thirty minutes, and then reached the growth temperature of 850° C after that. The growth temperature of 850° C was chosen because of the success of other samples grown at and near this temperature. The temperature was then held for fifteen to thirty minutes and then cooled naturally back to room temperature. All experiments used argon as a carrier gas with a flow rate of around 200 sccm (standard cubic centimeters per minute). Each sample was grown at 25kPa above atmospheric pressure. 25kPa was chosen as the pressure because the pressure in the system deters the molybdenum disulfide crystals from forming multiple layers or growing vertically. The crucible of elemental sulfur was placed in the tube so that sulfur gas would be flowing through the tube when the system reached growth temperature. The most important variable of this growth is the distance of the molybdenum(VI) oxide from the center. This changes the amount of evaporated molybdenum during the growth temperature due to the different temperature zones.

Figure 19 shows the Raman spectrum of a sample grown with the crucible of molybdenum(VI) oxide powder next to, and upwind of the blank sample (1 cm from the center of the tube) grown for 15 min. While the molybdenum disulfide was created, the result was a thick, amorphous film. It was so thick that the silicon peak was not present in

the spectrum. Figure 20 show the Raman spectrum of a sample grown with the crucible of molybdenum(VI) oxide powder next to, and downwind of the elemental sulfur powder grown (17.25 cm from the center of the tube) for 15 min. The result was very little, not significant growth that was not visible with an optical microscope. Figure 21 show the Raman spectrum of a sample grown with the crucible of molybdenum(VI) oxide powder around 15.25 cm (6 in) upwind of the blank sample in the center of the tube (shown in Figure 23) grown for 15 min. The result was small molybdenum disulfide crystals throughout the sample, but not continuous. Figure 22 show the Raman spectrum of a sample grown with the crucible of molybdenum(VI) oxide powder in the same position as the previous sample, around 15.25 cm (6 in) upwind of the blank sample in the center of the tube (shown in Figure 23), grown for 30 min instead of 15 min. The result was larger molybdenum disulfide crystals throughout the sample, but not continuous. An area of a sample grown using this method is shown in Figure 24, a photograph from an optical microscope at 50x. Table 4 is a table showing the locations of the E_{2g}^1 and A_{1g} peaks along with the difference between them (A_{1g}- E_{2g}^1) for each sample.

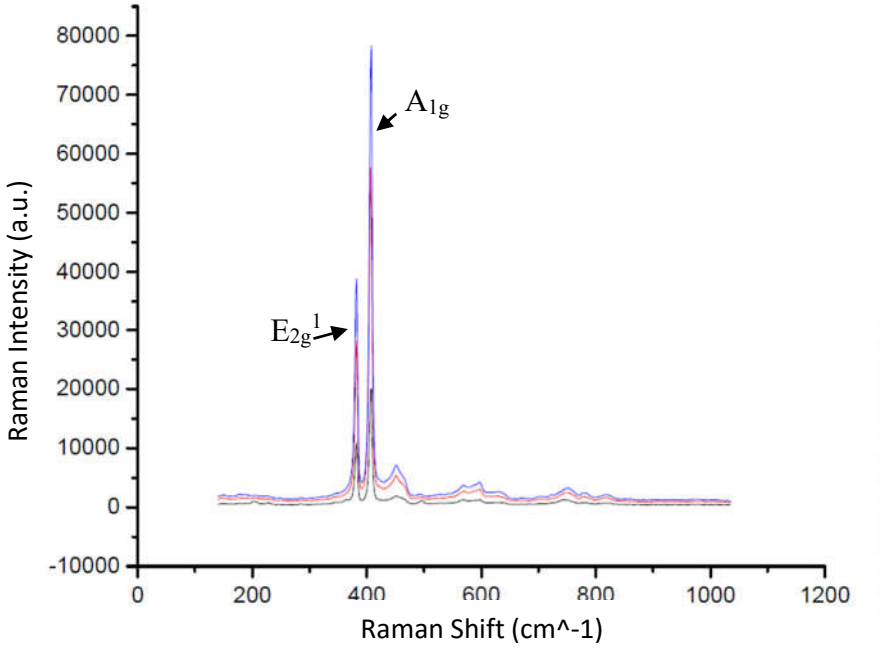

Figure 19. Raman spectrum of MoS_2 sample grown at 850° C for 15 minutes with MoO_3 powder near center temperature zone.

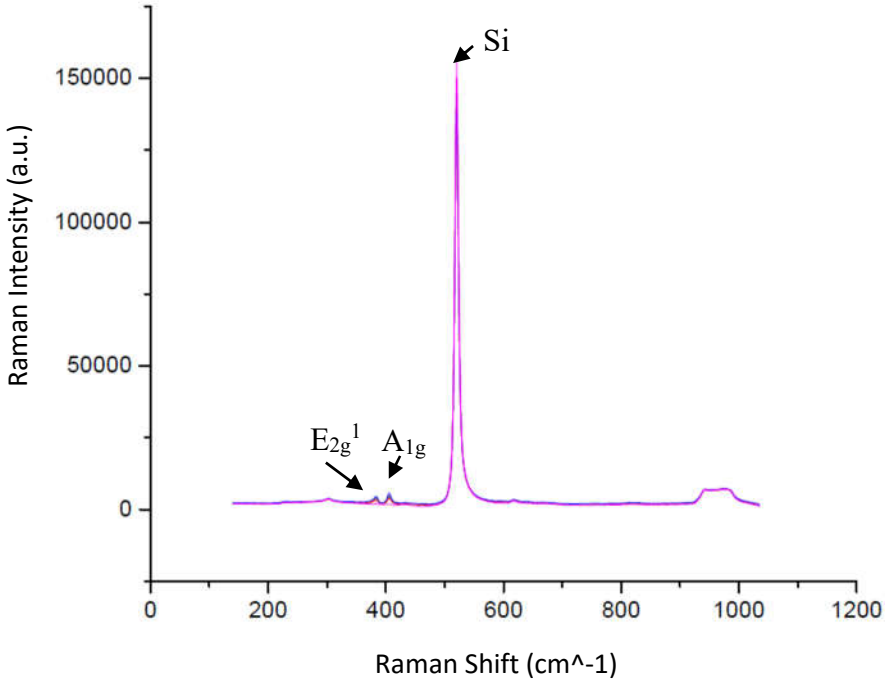

Figure 20. Raman spectrum of MoS_2 sample grown at 850° C for 15 minutes with MoO_3 powder in a low temperature zone.

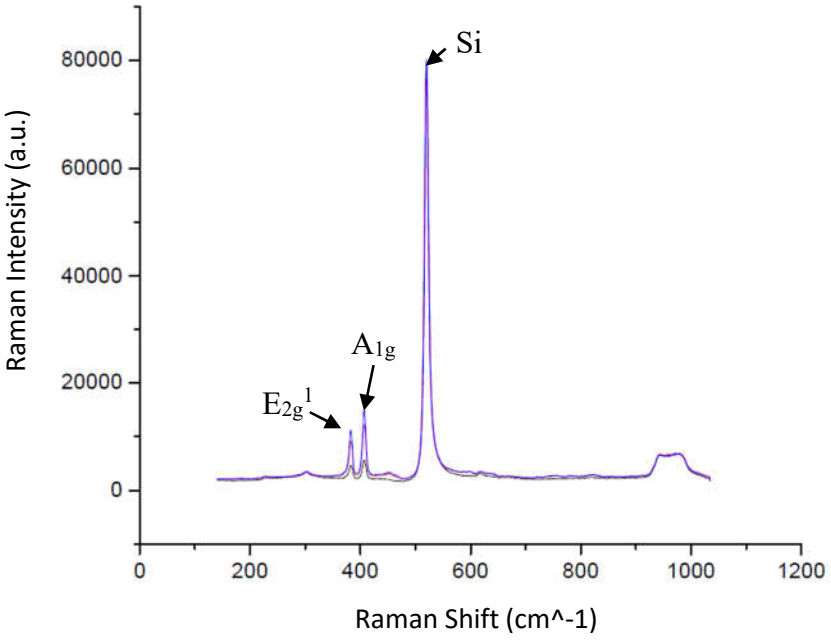

Figure 21. Raman spectrum of MoS_2 sample grown at 850° C for 15 minutes with MoO_3 powder in a lower temperature zone.

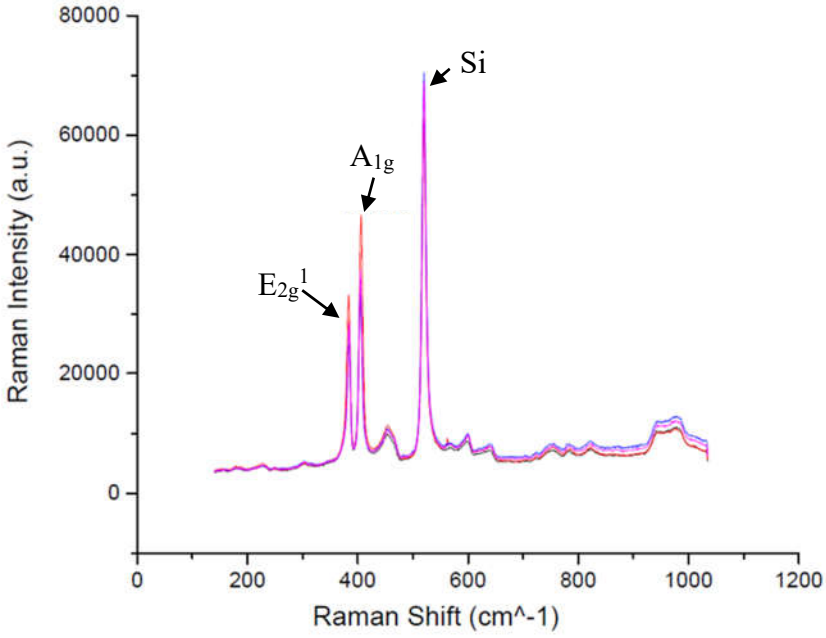

Figure 22. Raman spectrum of MoS_2 sample grown at 850° C for 30 minutes with MoO_3 powder in a lower temperature zone.

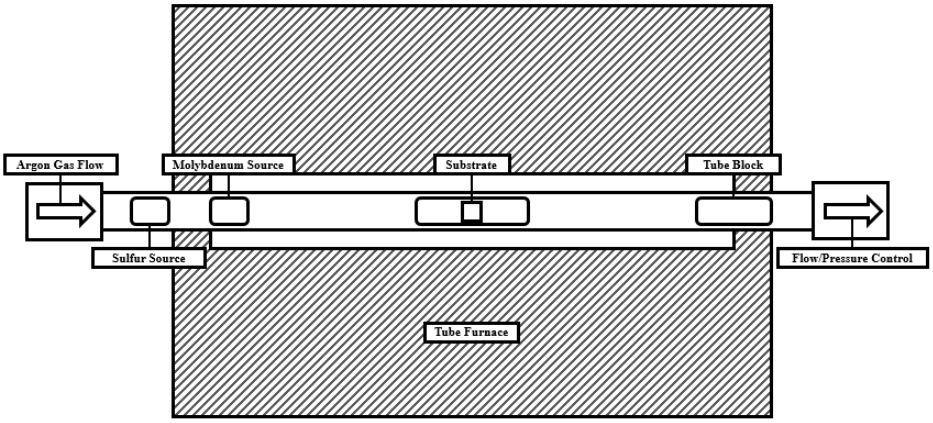

Figure 23. Optimal system setup for the MoO_3 powder method.

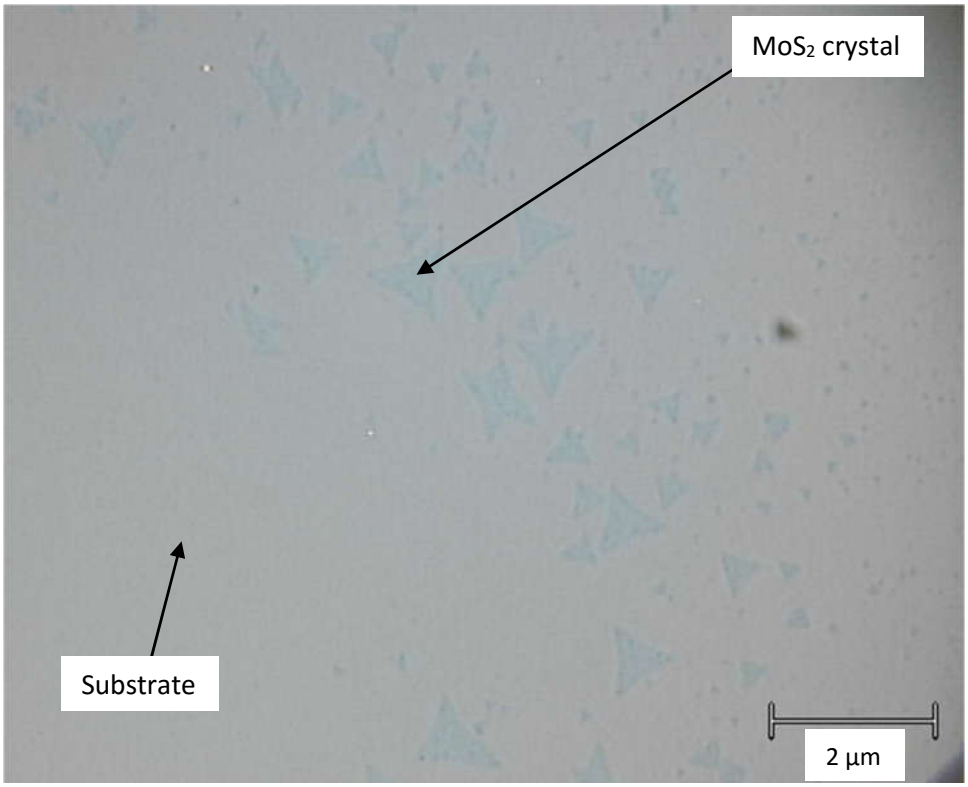

Figure 24. Photo of MoS_2 sample grown at 850° C for 30 minutes with MoO_3 powder in a lower temperature zone from an optical microscope.

MoO_3 Dist. From Center (cm)	E_{2g}^1 Location (cm^{-1})	A_{1g} Location (cm^{-1})	Difference (cm^{-1})
1	382.233	409.397	27.164
17.25	383.955	406.328	22.373
15.25 (for 15 min)	382.339	406.312	23.973
15.25 (for 30 min)	383.939	404.716	20.777

Table 4. Raman peak locations for MoS_2 samples grown by MoO_3 powder method.

This method proved to be a complex and somewhat repeatable way to synthesize crystals of molybdenum disulfide onto the surface of a substrate. Even for the best samples created, the nucleation sites of the molybdenum disulfide crystals were spread out and they were few in numbers. From the Raman spectrums and the peak differences, it can be determined that samples grown when the molybdenum(VI) oxide powder was 1cm away from the sample grew a very thick film where the peak difference was 27.164cm^{-1} and the substrate's Raman peak at 520cm^{-1} is not discernable, and the film grown 17.25cm 15.25cm away from the powder were much thinner. The samples grown at 15.25cm for 30min grew the largest crystals, having edges of up to 2μm, shown in Figure 24, that are monolayer, shown by the peak difference of 20.777cm^{-1}. The crystals grown with this method are triangular, as shown in Figure 24, because of the hexagonal lattice structure of molybdenum disulfide, and are oriented randomly, due to the amorphous nature of the SiO_2 surface. There are also multiple peaks within the Raman spectrums that are not specific to molybdenum disulfide or silicon, this shows that there

are other impurities within the synthesized films. In conclusion, a simple exploration into this method showed somewhat repeatable, very discontinuous, single crystals and polycrystals of triangular, single layer molybdenum disulfide that was highly affected by the temperature of the source materials.

CHAPTER IV

FUTURE WORK

Two-dimensional electronics has gathered a lot of interest in recent years. The procedure of these materials seems to go from discover, to analysis from bulk materials, to synthesis of films, to practical use. For practical use, two-dimensional films must be able to be synthesized easily and consistently. One of the two-dimensional materials that is currently in the process of finding simple synthesis methods is molybdenum disulfide. Molybdenum disulfide has been researched quite a bit since it's discover and, with the properties found from bulk samples, seems like it could have many practical applications for electronics. Before molybdenum disulfide can be used practically in electronics, some hurdles still must be overcome. The largest issues facing synthesized molybdenum disulfide films for electronics are the crystal grain boundaries as well as keeping the growth to a single layer.

The grain boundaries present in synthesized films of molybdenum disulfide decrease the electron and hole transport throughout the film which will lower the power efficiency of a device made with this material. To overcome the issues presented by the grain boundaries, films must have less crystals synthesized. With a lower number of crystals in the film, to keep the continuity of the film, larger crystals must be grown. One possible solution to this might be the use of seeding promoters. Seeding promoters help encourage the growth of specific crystalline structures. By using the right seeding

promoter, films of molybdenum disulfide could be grown with larger crystals, and fewer grain boundaries.

Keeping molybdenum disulfide films to a single molecular layer is also very important, because of the direct bandgap at the monolayer. By changing and optimizing different growth parameters such as carrier gas, substrate, pressure, etc. two-dimensional growth of molybdenum disulfide can be encouraged while three-dimensional or multilayer growth can be suppressed. The biggest difficulty surrounding this issue is the delicate balance of the source materials, finding the exact right source content to consistently create only single layers of molybdenum sulfide crystals.

In conclusion, to introduce molybdenum disulfide into electronics applications, a few more strides must be made. Once a method of monolayer molybdenum disulfide films that is found to be highly repeatable with favorable qualities, this material could be introduced to make large technological advances.

REFERENCES

[1] Geim, A. K., and K. S. Novoselov. "The Rise of Graphene." *A Collection of Reviews from Nature Journals Nanoscience and Technology* (2009): 11-19. Web.

[2] Geim, A. K. "Graphene: Status and Prospects." *Science* 324.5934 (2009): 1530-534. Web.

[3] Neto, A. H. Castro, F. Guinea, N. M. R. Peres, K. S. Novoselov, and A. K. Geim. "The Electronic Properties of Graphene." *Reviews of Modern Physics Rev. Mod. Phys.* 81.1 (2009): 109-62. Web.

[4] Wang, Qing Hua, Kourosh Kalantar-Zadeh, Andras Kis, Jonathan N. Coleman, and Michael S. Strano. "Electronics and Optoelectronics of Two-dimensional Transition Metal Dichalcogenides." *Nature Nanotech Nature Nanotechnology* 7.11 (2012): 699-712. Web.

[5] Wu, Wei, Debtanu De, Su-Chi Chang, Yanan Wang, Haibing Peng, Jiming Bao, and Shin-Shem Pei. "High Mobility and High On/off Ratio Field-effect Transistors Based on Chemical Vapor Deposited Single-crystal MoS_2 Grains." *Appl. Phys. Lett. Applied Physics Letters* 102.14 (2013): 142106. Web.

[6] Jin, Wencan, Po-Chun Yeh, Nader Zaki, Datong Zhang, Jerzy T. Sadowski, Abdullah Al-Mahboob, Arend M. Van Der Zande, Daniel A. Chenet, Jerry I. Dadap, Irving P. Herman, Peter Sutter, James Hone, and Richard M. Osgood. "Direct Measurement of the Thickness-Dependent Electronic Band Structure of MoS_2

Using Angle-Resolved Photoemission Spectroscopy." *Phys. Rev. Lett. Physical Review Letters* 111.10 (2013): n. pag. Web.

[7] Mak, Kin Fai, Changgu Lee, James Hone, Jie Shan, and Tony F. Heinz. "Atomically Thin MoS_2: A New Direct-Gap Semiconductor." *Phys. Rev. Lett. Physical Review Letters* 105.13 (2010): n. pag. Web.

[8] "Moore's Law." *Encyclopedia Britannica Online*. Encyclopedia Britannica, n.d. Web.

[9] Keyes, Robert W. "Physical Limits of Silicon Transistors and Circuits." *Rep. Prog. Phys. Reports on Progress in Physics* 68.12 (2005): 2701-746. Web.

[10] Ma, Lu, Digbijoy N. Nath, Edwin W. Lee, Choong Hee Lee, Mingzhe Yu, Aaron Arehart, Siddharth Rajan, and Yiying Wu. "Epitaxial Growth of Large Area Single-crystalline Few-layer MoS2 with High Space Charge Mobility of 192 Cm2 V 1 S 1." Appl. Phys. Lett. Applied Physics Letters 105.7 (2014): 072105. Web.

[11] Lee, Yi-Hsien, Xin-Quan Zhang, Wenjing Zhang, Mu-Tung Chang, Cheng-Te Lin, Kai-Di Chang, Ya-Chu Yu, Jacob Tse-Wei Wang, Chia-Seng Chang, Lain-Jong Li, and Tsung-Wu Lin. "Synthesis of Large-Area MoS 2 Atomic Layers with Chemical Vapor Deposition." Adv. Mater. Advanced Materials 24.17 (2012): 2320-325. Web.

[12] Li, X., W. Cai, J. An, S. Kim, J. Nah, D. Yang, R. Piner, A. Velamakanni, I. Jung, E. Tutuc, S. K. Banerjee, L. Colombo, and R. S. Ruoff. "Large-Area Synthesis of High-Quality and Uniform Graphene Films on Copper Foils." Science 324.5932 (2009): 1312-314. Web.

[13] “Lindberg/Blue M™ Mini-Mite™ Tube Furnaces” [Online]. Available: http://www.thermoscientific.com

[14] Najmaei, Sina, Zheng Liu, Wu Zhou, Xiaolong Zou, Gang Shi, Sidong Lei, Boris I. Yakobson, Juan-Carlos Idrobo, Pulickel M. Ajayan, and Jun Lou. "Vapour Phase Growth and Grain Boundary Structure of Molybdenum Disulphide Atomic Layers." Nature Materials Nat Mater 12.8 (2013): 754-59. Web.

[15] Green, Robert. “Hall Effect Measurements in Materials Characterization.” (2011). Web.

[16] Schroder, Dieter K. Semiconductor Material and Device Characterization. 3rd Ed. New York: John Wiley & Sons, 2006. Print.

[17] Zhang, Xin, Xiao-Fen Qiao, Wei Shi, Jiang-Bin Wu, De-Sheng Jiang, and Ping-Heng Tan. "Phonon and Raman Scattering of Two-dimensional Transition Metal Dichalcogenides from Monolayer, Multilayer to Bulk Material." Chem. Soc. Rev. 44.9 (2015): 2757-785. Web.

[18] Laskar, Masihhur R., Digbijoy N. Nath, Lu Ma, Edwin W. Lee, Choong Hee Lee, Thomas Kent, Zihao Yang, Rohan Mishra, Manuel A. Roldan, Juan-Carlos Idrobo, Sokrates T. Pantelides, Stephen J. Pennycook, Roberto C. Myers, Yiying Wu, and Siddharth Rajan. "P-type Doping of MoS2 Thin Films Using Nb." Appl. Phys. Lett. Applied Physics Letters 104.9 (2014): 092104. Web.